

# Parallel Conformal Hyperparameter Optimization

Riccardo Doyle

*London, UK*

R.DOYLE.EDU@GMAIL.COM

**Editor:**

## Abstract

Several novel frameworks for hyperparameter search have emerged in the last decade, but most rely on strict, often normal, distributional assumptions, limiting search model flexibility. This paper proposes a novel optimization framework based on upper confidence bound sampling of conformal confidence intervals, whose assumption of exchangeability enables greater choice of search model architectures. Several such architectures were explored and benchmarked on hyperparameter tuning of both dense and convolutional neural networks, displaying superior performance to random search.

**Keywords:** hyperparameter optimization, conformal prediction, deep learning

## 1. Introduction

Identifying optimal model parameters is deeply desirable for high prediction performance in machine learning, but challenging due to non-convexity and expensive search costs. Common approaches involving grid search - exhaustive iterative search of a confined parameter interval - or random search (Bergstra and Bengio, 2012) - random sampling from a broader parameter space – display complimentary weaknesses and form no expectation of hyperparameter performance ahead of search. Much focus has instead been placed on search frameworks involving pre-sampling inference, generally dominated by Sequential Model-Based Optimization, or SMBO (Hutter et al., 2011) – sequential training of a performance estimator on previously sampled hyperparameters to guide future sampling based on estimator expectations. Early applications (Hutter et al., 2011; Bergstra et al., 2011) found positive outperformance on expert consensus across a range of benchmarked datasets through Gaussian Process or Tree-structured Parzen estimators. Encouraging results promoted further research with additions involving search cost inclusion as an optimization criterion (Snoek et al., 2012), early forms of online resource allocation and distributed search (Swersky et al., 2013), unwanted parameter space pruning (Wistuba et al., 2015), or replacement of single estimators with ensemble methods (Lacoste et al., 2014), among others. Though alternative approaches have surfaced (Turner et al., 2021), SMBO-based search has become one of the most popular non-naïve search methods in the training of complex machine learning predictors, with frequent appearances in competitions (Turner et al., 2021) and package releases (Kandasamy et al., 2020). Its Bayesian architecture allows for rigorously constructed normally distributed confidence intervals and the prevalent use of Gaussian Processes as point estimators allows for flexible and inexpensive retraining, however while its impositions of normality are beneficial to validity, they restrict point estimators’ functional forms. In this

study we replace SMBO with a similarly structured, but less constraining, point-estimate and variance process with no reliance on normally distributed outputs. Specifically, SMBO’s commonplace Gaussian point estimators will be substituted with a choice of regression models and its normal confidence intervals with conformal prediction intervals limited only by assumptions of exchangeability. This approach retains the benefits of a fitted predictor and sequential framework, but offers wider flexibility in the choice of both point and variance estimators, allowing for more complex, and, expectantly, better fitting architectures.

## 2. Review of Conformal Prediction

Common hyperparameter sampling methods involving statistical optimization rely on confidence intervals to identify areas of high uncertainty. While robust, these bounds impose distributional assumptions on the data – often normality – resulting in a limited choice of models. As an alternative, in this section we introduce the concept of conformal prediction intervals.

### 2.1 Split Conformal Prediction (SCP)

For a given training set  $X_{train}, Y_{train} = \{(X_i, Y_i) | i \in I_{train}, I_{train} \not\subset I_{val}\}$  and validation set  $X_{val}, Y_{val} = \{(X_i, Y_i) | i \in I_{val}, I_{val} \not\subset I_{train}\}$ , let us calibrate a chosen point estimator model to the training set and generate the mapping function  $f(X_i) = \hat{Y}_i$ .

To construct a conformal prediction interval (Shafer and Vovk, 2008) for the estimator’s outputs, we must define some nonconformity function  $C(Y_i, \hat{Y}_i)$  quantifying the divergence between observed and model function-predicted outputs  $Y_i$  and  $\hat{Y}_i$ . Functional form is arbitrary and needs to satisfy only exchangeability of outputs. For simplicity we define this as the absolute deviation between observed and predicted outputs:

$$C(\hat{Y}_i, Y_i) = |Y_i - \hat{Y}_i| \quad (1)$$

We then obtain predicted outputs for all validation set observations  $\hat{Y}_{val} = f(X_{val})$ , which can be in turn passed jointly with their observed counterparts through the conformity scoring function to obtain a multiset of divergences  $D$ :

$$D = |Y_{val} - (\hat{Y}_{val})| \quad (2)$$

For a given confidence level  $\alpha$ , we now denote our conformal prediction interval on an unseen new test input  $X_{N+1}$  as:

$$CI(X_{N+1}) = [f(X_{N+1}) \pm q_{1-\alpha}(D)] \quad (3)$$

Where  $q_{1-\alpha}(D)$  is the  $1-\alpha$  quantile of the multiset  $D$ . Consequently, we state the probability bound with which a new  $Y_{N+1}$  label falls within our previously defined confidence interval as:

$$1 - \alpha + \frac{1}{(N - n) + 1} \geq P(Y_{N+1} \in CI(X_{N+1})) \geq 1 - \alpha \quad (4)$$

## 2.2 Locally Weighted Conformal Prediction (LWCP)

Prediction intervals formed with SCP produce  $X_i$  invariant interval width. This is not suited to SMBO inspired frameworks, as expected variance at each point is constant and search would be purely exploitative. This shortcoming can be addressed by weighing (Lei et al., 2018) the conformal score by some conditional variance estimator  $V(X_i)$ :

$$C(\hat{Y}_i, Y_i) = \frac{|\hat{Y}_i - Y_i|}{V(X_i)} \quad (5)$$

Resulting in an updated conformal interval of:

$$CI(X_{N+1}) = [f(X_{N+1}) \pm V(X_{N+1})q_{1-\alpha}(D)] \quad (6)$$

Such that higher variance or uncertainty expands the interval and lower variance contracts it, while still maintaining the same global coverage under exchangeability.  $V(X_i)$ 's outcome variable and functional form are arbitrary; any choice of regression estimator may be used and many choices of outcome variable would still guarantee overall conformal scores generated in equation 5 to be exchangeable. In this paper,  $V(X_i)$  is set to predict the mean absolute deviation of the point estimator's absolute errors, denoted below as  $v_i$ :

$$v_i = \left| \hat{Y}_i - Y_i \right| - \sum_{i=1}^N \frac{|\hat{Y}_i - Y_i|}{N} \quad (7)$$

Setting the variance estimator to predict the errors of the point estimator results in conformal intervals that expand and contract based on the point estimator's predictive accuracy, thus replicating the intervals of a more traditional Gaussian Process and counteracting heteroskedasticity. It is worth noting that if the variance estimator is predicting the errors of another estimator, the conformal fitting procedure differs slightly from that described in SCP, as additional care must be taken to avoid bias. To elaborate, we further partition the original  $X_{train}, Y_{train}$  set to produce two further indexed subsets  $X_1, Y_1 = \{(X_i, Y_i) | i \in I_1, I_1 \in I_{train}, I_1 \not\subset I_2\}$  and  $X_2, Y_2 = \{(X_i, Y_i) | i \in I_2, I_2 \in I_{train}, I_2 \not\subset I_1\}$ . The point estimator  $f(X_i) = \hat{Y}_i$  is first fitted on set  $X_1, Y_1$ . Its out of sample absolute errors are then produced using set  $X_2, Y_2$ , resulting in set  $E_2 = |\hat{Y}_2 - Y_2|$ . The variance estimator, in turn, is fitted on  $X_2$  to predict the mean absolute deviation of the point estimator's out of sample residuals  $|E_2 - \mu(E_2)|$ . This results in two fitted estimators which can now be used on the unchanged validation set to produce a multiset of conformal divergences:

$$D = \frac{|Y_{val} - f(Y_{val})|}{V(X_{val})} \quad (8)$$

Further splitting the original training set is necessary to avoid the variance estimator from training on in-sample point estimator errors, which are biased to the training data and thus distorted or understated.

## 2.3 Conformalized Quantile Regression (CQR)

Locally weighted approaches produce valid and adaptive conformal intervals suited to the purposes of this paper. Their only limitation is interval symmetry, which may overstate the

interval size required to obtain the same coverage where errors are either primarily positive or primarily negative. This is particularly relevant in the context of hyperparameter search where negative variance (consistently lower performance than point estimator predicted performance) is detrimental, but would increase chance of sampling with a symmetrical scorer. To remedy this, we introduce quantile regression (Koenker and Bassett, 1978). In its simplest linear form, quantile regression derives the coefficients  $\beta_j$  of some linear regression formula  $Y_i = \sum_{j=1}^p X_{i,j}\beta_j + e_i$  with a pinball loss function  $L_\alpha$ :

$$L_\alpha(u_i) = \begin{cases} u_i\alpha & \text{if } u_i > 0 \\ u_i(\alpha - 1) & \text{if } u_i \leq 0 \end{cases} \quad (9)$$

Where  $u_i$  is the absolute error between predicted and observed outputs  $u_i = |Y_i - \sum_{j=1}^p X_{i,j}\beta_j|$ . Regression parameters are then estimated according to the minimization:

$$\arg \min_{\beta_1 \dots \beta_j} \sum_{i:Y_i \geq \sum_{j=1}^p x_{i,j}\beta_j}^N \alpha u_i + \sum_{i:Y_i < \sum_{j=1}^p x_{i,j}\beta_j}^N (1 - \alpha) u_i \quad (10)$$

It can separately be shown that the  $\alpha$ -th quantile minimizes the above equation, resulting in a regressive estimator whose output per observation is a pre-specified upper or lower bound conditional on the desired confidence level and  $X$ , denoted hereafter simply as  $Q(X_i, \alpha)$ . A prediction interval for some new observation  $CI(X_{N+1})$  can then trivially be generated by fitting two quantile regression estimators for some pre-specified symmetrical upper and lower bound  $1 - \alpha$  and  $\alpha$ , with the predictions of each regression forming the bounds of the interval:

$$CI(X_{N+1}) = [Q(X_{N+1}, 1 - \alpha), Q(X_{N+1}, \alpha)] \quad (11)$$

This interval, though useful in practice, does not provide coverage guarantees on unseen data. To improve robustness, let us extend the interval generating process using conformalization (Romano et al., 2019). We begin by echoing previous steps and fit two quantile estimators,  $Q(X_{N+1}, 1 - \alpha)$  and  $Q(X_{N+1}, \alpha)$ , on some training data  $X_{train}, Y_{train}$ . A choice of non-conformity score is then required to evaluate model outputs. In line with existing literature (Romano et al., 2019) and given guarantees of exchangeability, we produce deviations on a validation set  $X_{val}, Y_{val}$  using the following non-conformity score:

$$D = \max(Q(X_{val}, 1 - \alpha) - Y_{val}, Y_{val} - Q(X_{val}, \alpha)) \quad (12)$$

A conformal prediction interval can then be obtained by adjusting the initial quantile estimates by the  $1 - \alpha$  and  $\alpha$  quantiles of the multiset of validation deviations  $D$ :

$$CI(X_{N+1}) = [Q(X_{N+1}, 1 - \alpha) - q_{1-\alpha}(D), Q(X_{N+1}, \alpha) + q_{1-\alpha}(D)] \quad (13)$$

Note the  $\alpha$  term on the initial quantile regression estimators and the  $\alpha$  term on the conformal interval need not be the same, but they are set to be the same in this paper for search consistency.

### 3. Parallel Conformal Hyperparameter Optimization (PCHO)

Let  $X_j, Y_j$  be some labelled set used to fit some machine learning model with architecture  $\Theta$ . Further let  $\{\theta_t\}_{t=1}^T$  be some finite set of randomly combined hyperparameter configurations, where each  $\theta_t$  is a full configuration containing an assigned value for each hyperparameter in  $\Theta$ .

Let us then initiate a naive parallel search framework by producing  $m$  equal length batches  $X_i^m, Y_i^m$  of bootstrapped  $X_j, Y_j$  pairs – where batch size is a free parameter. Further split each batch into training and validation partitions:

$$X_{train}^m, Y_{train}^m = \{(X_i^m, Y_i^m) | i \in I_{train}^m, I_{train}^m \not\subset I_{val}^m\} \quad (14)$$

$$X_{val}^m, Y_{val}^m = \{(X_i^m, Y_i^m) | i \in I_{val}^m, I_{val}^m \not\subset I_{train}^m\} \quad (15)$$

Randomly sample  $m$  configurations without replacement from  $\{\theta_t\}_{t=1}^T$  and fit a model with chosen architecture  $\Theta$  on each batch and configuration pair, generating  $m$  fitted models  $f_m(X) \mapsto \hat{Y}$ :

$$f_m(X) \leftarrow \Theta(X_{train}^m, Y_{train}^m, \theta_m) \quad (16)$$

Taking some undefined loss function  $L(Y, f(X))$ , evaluate the out of sample error in each  $f_m(X)$ 's outputs and define the loss incurred by each configuration  $\theta_m$  to be:

$$l_m = L(Y_{val}^m, f_m(X_{val}^m)) \quad (17)$$

Remaining methodology will outline the application of Locally Weighted Conformal Prediction, though it should be apparent how Conformalized Quantile Regression can be applied instead.

To expand, produce a secondary labelled set consisting of hyperparameter configurations and associated validation loss values  $\theta_m, l_m$ . Further split this set into training and validation partitions:

$$\theta_{train}, l_{train} = \{(\theta_m, l_m) | m \in M_{train}, M_{train} \not\subset M_{val}\} \quad (18)$$

$$\theta_{val}, l_{val} = \{(\theta_m, l_m) | m \in M_{val}, M_{val} \not\subset M_{train}\} \quad (19)$$

Then further split the training set into two additional sub-partitions as outlined in Section 2.2:

$$\theta_{train'}, l_{train'} = \{(\theta_m, l_m) | m \in M_{train'}, M_{train'} \in M_{train}, M_{train'} \not\subset M_{val'}\} \quad (20)$$

$$\theta_{val'}, l_{val'} = \{(\theta_m, l_m) | m \in M_{val'}, M_{val'} \in M_{train}, M_{val'} \not\subset M_{train'}\} \quad (21)$$

Now fit some machine learning model with architecture  $\lambda$  on the first sub partition of the training data, producing a fitted model  $g(\theta) \mapsto \hat{l}$ :

$$g(\theta) \leftarrow \lambda(\theta_{train'}, l_{train'}) \quad (22)$$

This model acts as a point estimator providing an expectation of the loss associated with each hyperparameter in model architecture  $\Theta$  when trained on similar data to that in equation (16). To produce locally weighted intervals for its predictions, as outlined in previous

methodology sections, we train a separate machine learning model with architecture  $\tau$  (this may or may not be the same architecture as the point estimator) to predict the variability  $v$  of its errors conditional on  $\theta$ . Variability is defined by the mean absolute deviation of the point estimator's absolute errors and is obtained from the second sub partition of the training data to avoid bias (as point estimator errors will be small or morphed if obtained from the same data used to fit it):

$$v_{val'} = ||g(\theta_{val'}) - l_{val'}| - \mu(|g(\theta_{val'}) - l_{val'}|) \quad (23)$$

The variability estimator can then be fit on second sub partition data to produce a fitted model  $h(\theta) \mapsto \hat{v}$ :

$$h(\theta) \leftarrow \tau(\theta_{val'}, v_{val'}) \quad (24)$$

With both estimator functions fitted, we can define a general non conformity score quantifying the model's variance weighted errors as:

$$C(\hat{l}, \hat{v}, l) = \frac{|l - \hat{l}|}{\hat{v}} \quad (25)$$

Which when applied to the validation set can be used to produce the set of divergences  $D$ :

$$D = \frac{|l_{val} - g(\theta_{val})|}{h(\theta_{val})} \quad (26)$$

That in turn can be used to generate the following final adaptive conformal interval for any of  $h(\theta)$ 's predictions given a specified confidence level  $\alpha$ :

$$CI(h(\theta)) = [Q(h(\theta), 1 - \alpha) - q_{1-\alpha}(D), Q(h(\theta), \alpha) + q_{1-\alpha}(D)] \quad (27)$$

We now have a point estimator  $h(\theta)$  capable of producing confidence bounded predictions for the loss on architecture  $\Theta$  corresponding to any hyperparameter configuration in  $\{\theta_t\}_{t=1}^T$  (note that for configurations that have already been sampled the confidence bounds equal the observed value). Lower bound estimates of performance at each configuration can then be obtained from  $LB_t = Q(h(\{\theta_t\}_{t=1}^T), 1 - \alpha) - q_{1-\alpha}(D)$  and we can select the best performing configuration to test on full, non-batched data using an Upper Confidence Bound (UCB) framework selecting the configuration corresponding to the smallest lower bound in the set (or largest upper bound if using positively directional metrics like accuracy instead of loss):

$$\theta_{best} = \arg \min_{\theta} (LB_t) \quad (28)$$

This results in the original model with architecture  $\Theta$  being fitted on its full training set as:

$$f(X) \leftarrow \Theta(X_{train}, Y_{train}, \theta_{best}) \quad (29)$$

With an associated final validation loss of  $L(Y_{val}, f(X_{val}))$ . It is worth highlighting that conformal intervals will be most accurate for models trained on the same data size as the batches that produced them. The application of conformal intervals trained on batch data to model performance trained and evaluated on full data can be viewed as two parallel processes, where the outputs of one process are used to guide the sampling of the other, assuming

---

**Algorithm 1** Parallel Conformal Hyperparameter Optimization (PCHO)

---

**Require:**  $MAD(l) = |l_i - \mu(l)|$ ,  $MSE(Y, \hat{Y}) = \frac{1}{n} \sum_{i=1}^n (Y_i - \hat{Y}_i)^2$

- 1:  $X_{train}, X_{val}, Y_{train}, Y_{val} \leftarrow train\_val\_split(X, Y)$
- 2:  $\theta_{space} = \{\theta_t\}_{t=1}^T$
- 3:  $P = [], L = []$
- 4: **for**  $k = 1 : max\_iter$  **do**
- 5:   **if**  $k - k_{last\_batched} > retrain\_interval$  **then**
- 6:      $k_{last\_batched} = k$
- 7:     **for**  $m = 1 : batch\_number$  **do**
- 8:        $\theta_m \leftarrow random.choose(from = \theta_{space}, where = \theta_m \not\in P)$
- 9:        $X^m, Y^m \leftarrow bootstrap(from = X, Y)$
- 10:        $X_{train}^m, X_{val}^m, Y_{train}^m, Y_{val}^m \leftarrow train\_val\_split(X^m, Y^m)$
- 11:        $(f_m : X \mapsto \hat{Y}) \leftarrow \Theta(X_{train}^m, Y_{train}^m, \theta_m)$
- 12:        $l_m \leftarrow MSE(f(X_{val}^m), Y_{val}^m)$
- 13:        $L.append(l_m)$
- 14:        $P.append(\theta_m)$
- 15:     **end for**
- 16:   **end if**
- 17:    $P_{train}, P_{val}, L_{train}, L_{val} \leftarrow train\_val\_split(P, L)$
- 18:    $P_{train'}, P_{val'}, L_{train'}, L_{val'} \leftarrow train\_val\_split(P_{train}, L_{train})$
- 19:    $(g : \theta \mapsto \hat{l}) \leftarrow \Lambda(P_{train'}, L_{train'})$
- 20:    $(h : \theta \mapsto MAD(l)) \leftarrow \tau(P_{val'}, MAD(MSE(g(P_{val'}), L_{val'})))$
- 21:    $D = \frac{|L_{val} - g(P_{val})|}{V(P_{val})}$
- 22:    $l_{lower\_bounds} = g(\theta_{space}) - h(\theta_{space})q_{1-\alpha}(D)$
- 23:    $\theta_{best} = \arg \min_{\theta} (l_{lower\_bounds})$
- 24:    $(f : X \mapsto \hat{Y}) \leftarrow \Theta(X_{train}, Y_{train}, \theta_{best})$
- 25:    $l_{best} = MSE(f(X_{val}), Y_{val})$
- 26:   **if**  $l_{best} < best\_search\_loss$  **then**
- 27:      $best\_search\_loss = l_{best}$
- 28:      $best\_parameter\_configuration = \theta_{best}$
- 29:   **end if**
- 30: **end for**

---

some degree of proportionality between the two. For a large enough batch, depending on model complexity and minimum data required to obtain meaningful performance, the two should converge.

Above steps constitute a single PCHO iteration and are repeated fully at every subsequent iteration with one methodological difference. When new loss values are produced from a successive iteration's batches in equation 17, the resulting new configuration and loss pairs  $\theta, l$  are appended to the previous iterations' existing pairs. Remaining steps are then carried out on this joined and expanded set rather than the standalone sets produced in each iteration. The expansion produces a bigger and richer training set for the conformal point and variance estimator models as search progresses. A summary of above steps can be found in Algorithm 1.

In addition to aforementioned statistical frameworks, PCHO was enriched with optimization parameters to improve real world performance. Among the most relevant are (1) adaptive batch number sizing and (2) retraining intervals: (1) Adaptive batch sizing involves allocating a larger number of batches to PCHO’s first iteration, with a smaller number for subsequent iterations. This guarantees there is enough batch data to train conformal estimators, but doesn’t enforce the same high computational cost associated with higher batch numbers for subsequent incremental iterations. (2) Retraining intervals specify whether following each PCHO iteration, a subsequent one should immediately be triggered, or whether the same trained point and variance estimators can be used to keep sampling full data configurations, transforming equation 28’s best parameter criterion, to a best  $N$  parameter criterion, where  $N$  is the retraining interval.

Lastly, to comment on theoretical coverage and assumptions, all conformal intervals generated via PCHO provide guarantees of validity assuming conformal scores are exchangeable. Hyperparameter configurations between PCHO iterations are sampled randomly with replacement from a parent configuration set, making them dependant but exchangeable. Likewise the sequence of losses corresponding to a random seeded machine learning model using each configuration on a given batch is exchangeable. It is then reasonable to assume conformal scores generated by taking the difference between a configuration’s loss  $l_m$  and its predicted loss  $f(\theta_m)$  – obtained from some deterministic transformation of the inputted configuration  $\theta_m$  following the fitting of a point estimator model – are likewise exchangeable, resulting in reliable confidence intervals for search as of each iteration.

## 4. Benchmarking and Results

### 4.1 PCHO Performance on Dense Artificial Neural Network (DNN)

Performance is first tested on the parameters of a dense fully connected artificial neural network with a searchable hyperparameter space comprised of 10,000 randomly generated combinations of individual parameter values reported in Table 1. We consider two benchmark classification datasets; UCI’s Census Income dataset (CENSUS) (Dua and Graff, 2023) and Figure Eight’s Twitter US airline sentiment analysis dataset (TSA) (Figure Eight).

Hyperparameter	Search Value
Solver	[Adam, SGD]
Learning Rate	[0.00001, 0.0001, 0.001, 0.005, 0.01, 0.05, 0.1]
Alpha Regularization	[0.00001, 0.0001, 0.001, 0.005, 0.01, 0.05, 0.1, 0.5, 1, 3, 10]
Nodes in Given Layer	[4, 8, 16, 32, 56, 60, 80, 100, 120, 140]
Number of Layers	[2, 3, 4, 5]

Table 1: Individual hyperparameter values of searchable hyperparameter space for dense fully connected artificial neural network.

Optimization performance of several PCHO variations alongside random search (RS) on the CENSUS dataset can be found in the left panel of Figure 1. Validation accuracy of the model being hyperparameter searched is plotted over search runtime for two locally

weighted (LW) conformal variants and one conformalized quantile regression (QR) variant. LW variants are tested with either a gradient boosted (GBM) or random forest (RF) point and variance estimator architecture, while the QR variant utilizes a gradient boosted architecture. We note overall conformal performance is positive, with all three PCHO variants achieving a higher validation accuracy than random search. Highest end of run performance was achieved by the quantile regression variant (QR GBM) with validation accuracy of 82.85% compared to random search's 82.61% (Table A1, Appendix A).

Quality of uncertainty estimation differed by variant, with conformal interval breach rates on a batch of bootstrapped data of equal size to that used for training of the conformal search framework ranging from 10.34% to 27.41% (Table A1, Appendix A), against a theoretical target of 20% (given a confidence level choice of 80% for all variants in this simulation). All variants performed reasonably closely to the theoretical benchmark, though LW GBM performed most robustly. Standalone quality of point estimation is summarized in the right panel of Figure 1. For simplicity, only locally weighted variants were analysed in this plot. Mean absolute error (MAE) on each LW point estimator's validation folds is reported over time, with each marker indicating a new retraining event of the estimator (occurring every 5 search iterations, as this was the selected conformal retraining interval of this simulation). We note the RF estimator performs marginally better than the GBM estimator, with both improving in detection performance as search progresses, which validates the utility of appending incremental batched configuration and loss pairs at each PCHO iteration.

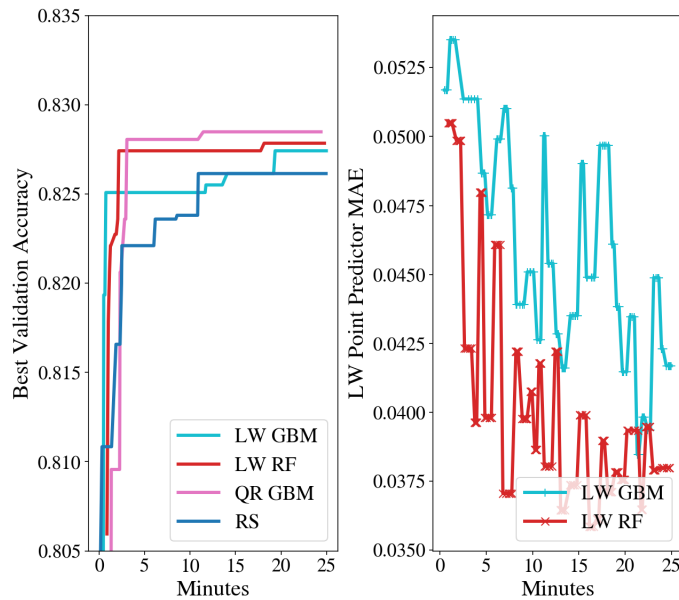


Figure 1: Best validation accuracy of DNN model tuned on CENSUS data through either PCHO or random search (RS). Lines correspond to best accuracy achieved at each minute of search time by random search and various locally weighted (LW) and quantile regression (QR) variants of the PCHO algorithm at 80% confidence.

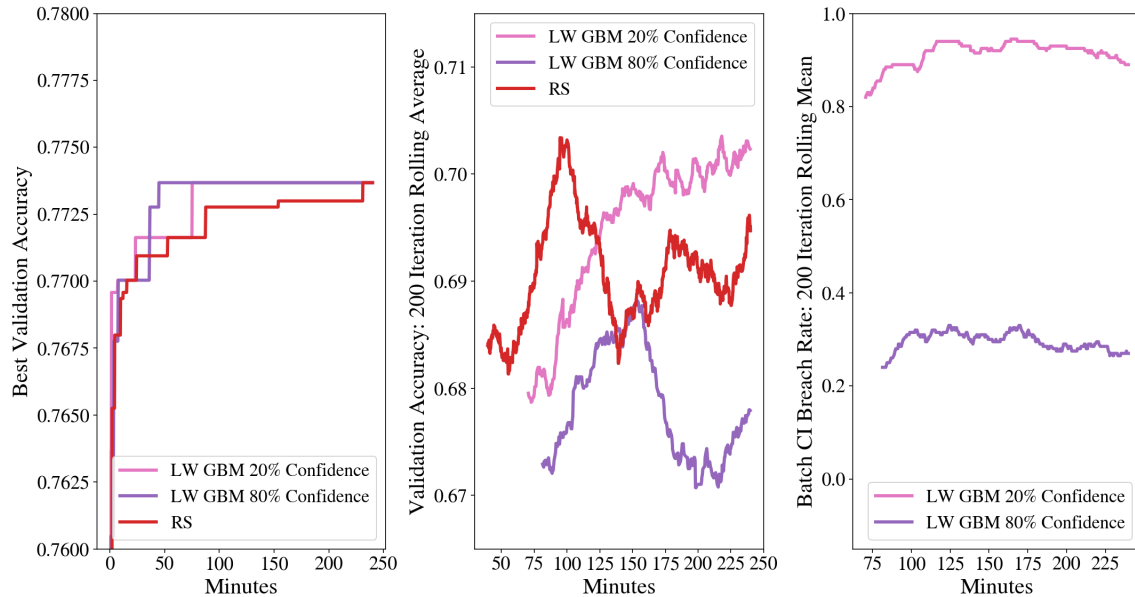


Figure 2: From left to right, all plotted over search runtime: [1] Best validation accuracy of DNN model tuned on TSA data through a 20% and 80% confidence LW GBM PCHO framework and random search (RS). [2] 200 search iteration rolling average of sampled parameter accuracies of DNN model tuned through previously specified PCHO variants and random search [3] 200 search iteration rolling conformal confidence interval (CI) breach rate on batched data (of same size as PCHO training batches) across previously specified PCHO variants and RS.

Results of a second benchmark testing the impact of confidence interval width on the TSA dataset are reported in Figure 2. A single LW GBM configuration was run at 20% and 80% confidence levels, with both substantially outperforming random search over the course of the simulation, but converging to the same best validation accuracy of 77.37% (Table A2, Appendix A). Choice of confidence level did not meaningfully affect search performance, but did affect search path. Smaller confidence intervals from the LW GBM 20% configuration resulted in greedier search with an average validation accuracy per PCHO iteration of 69.35% compared to the more variance oriented 80% configuration's 67.86% (Table A2, Appendix A). Breach rates for both confidence configurations were close to their theoretical levels, with the LW GBM 20% configuration achieving 87.73% breach rate and the 80% configuration achieving 26.85% (Table A2, Appendix A).

## 4.2 PCHO Performance on Convolutional Neural Network (CNN)

We further test our methodology on a convolutional neural network (CNN) architecture to validate performance on a more complex configuration of parameters, this time comprised of 10,000 randomly generated combinations of individual parameter values reported in Table 2. We consider four benchmarking classification datasets: the MNIST digit recognition dataset (Keras, c), the FMNIST clothes recognition dataset (Keras, b), and the CIFAR10 object detection dataset (Keras, a).

Hyperparameter	Search Value
Solver	[Adam, SGD]
Learning Rate	[0.0001, 0.0005, 0.001, 0.005, 0.01, 0.05]
Drop Out Rate	[0.1, 0.2, 0.3, 0.4, 0.5, 0.6, 0.7, 0.8, 0.9]
Number of Convolutions in Given Layer	[16, 32, 48 .. 256]
Number of Layers	[2, 3, 4]
First Dense Layer: Number of Neurons	[100, 200, 512]
Second Dense Layer: Number of Neurons	[0, 50, 100]

Table 2: Individual hyperparameter values of searchable hyperparameter space for convolutional neural network.

Search performance of a default LW GBM variant of the PCHO algorithm at 20% confidence compared to random search on this section’s three benchmark datasets can be found in Fig. 3. We note PCHO performance is once again superior to its random counterpart, with PCHO achieving higher end of simulation accuracy in all tested datasets. The greatest improvement was observed in the FMNIST dataset, with a final PCHO validation accuracy of 91.54% compared to random search’s 90.86% (Table A3, Appendix A). Average validation accuracy over runtime was significantly higher in PCHO configurations than random search, and significantly higher than in previous DNN simulations. This can be attributed to the increased complexity of convolutional hyperparameters and the need for expertly aggregated complementary combinations to produce passable performance. The most notable such divergence was observed in CIFAR10, with an average PCHO validation accuracy of 70.69% to random search’s 42.80% (Table A3, Appendix A). It is worth noting sampling more complex hyperparameter configurations in this instance only resulted in a modest increase in runtime costs, with an average search iteration duration of 1241.2 seconds under PCHO compared to 1084.8 under random search (Table A3, Appendix A). Lastly conformal uncertainty estimation remained adequate, with batched confidence interval breach rates ranging from 82.67% to 91.67% across all convolutional datasets (Table A3, Appendix A). Sound PCHO performance can thus be observed on both DNN and CNN model architectures.

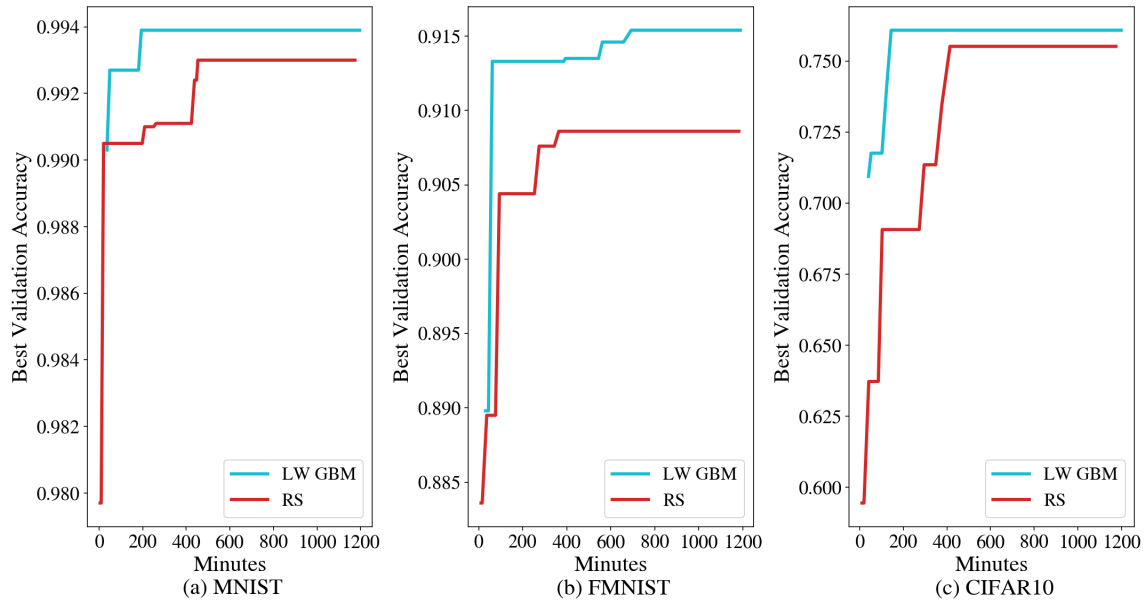


Figure 3: Best validation accuracy of DNN model tuned on suite of CNN datasets through either a 20% confidence LW GBM variant of PCHO or random search (RS).

## 5. Conclusion

This study introduced a novel optimization framework for hyperparameter selection based on parallel conformal prediction. Performance across a range of benchmarked datasets spanning tabular classification, sentiment analysis and image recognition was superior to random search in both final accuracy achieved and time to achievement. Empirical validity of conformal intervals was sound, with most displaying acceptable or negligible divergences from their theoretical bounds on batched samples. Further performance improvements could be achieved with the introduction of early stopping logic based on expected improvement inference and the inclusion of expected search cost in acquisition function design.

## References

- James Bergstra and Yoshua Bengio. Random search for hyper-parameter optimization. *Journal of Machine Learning Research*, 13(10):281–305, 2012. URL <http://jmlr.org/papers/v13/bergstra12a.html>.
- James Bergstra, Rémi Bardenet, Yoshua Bengio, and Balázs Kégl. Algorithms for hyper-parameter optimization. In J. Shawe-Taylor, R. Zemel, P. Bartlett, F. Pereira, and K.Q. Weinberger, editors, *Advances in Neural Information Processing Systems*, volume 24. Curran Associates, Inc., 2011. URL <https://proceedings.neurips.cc/paper/2011/file/86e8f7ab32cf12577bc2619bc635690-Paper.pdf>.
- Dheeru Dua and Casey Graff. UCI machine learning repository, 2023. URL <https://archive.ics.uci.edu/ml/datasets/census+income>.
- Figure Eight. Twitter us airline sentiment. URL <https://www.kaggle.com/datasets/crowdflower/twitter-airline-sentiment>.
- Frank Hutter, Holger H. Hoos, and Kevin Leyton-Brown. Sequential model-based optimization for general algorithm configuration. *International Conference on Learning and Intelligent Optimization*, pages 507–523, 2011.
- Kirthevasan Kandasamy, Karun Raju Vysyaraju, Willie Neiswanger, Biswajit Paria, Christopher R. Collins, Jeff Schneider, Barnabas Poczos, and Eric P. Xing. Tuning hyperparameters without grad students: Scalable and robust bayesian optimisation with dragonfly. *Journal of Machine Learning Research*, 21(81):1–27, 2020. URL <http://jmlr.org/papers/v21/18-223.html>.
- Keras. Cifar10 small images classification dataset, a. URL <https://keras.io/api/datasets/cifar10/>.
- Keras. Fashion mnist dataset, an alternative to mnist, b. URL [https://keras.io/api/datasets/fashion\\_mnist/](https://keras.io/api/datasets/fashion_mnist/).
- Keras. Mnist digits classification dataset, c. URL <https://keras.io/api/datasets/mnist/>.
- Roger Koenker and Gilbert Bassett. Regression quantiles. *Econometrica*, 46(1):33–50, 1978. ISSN 00129682, 14680262. URL <http://www.jstor.org/stable/1913643>.
- Alexandre Lacoste, Hugo Larochelle, François Laviolette, and Mario Marchand. Sequential model-based ensemble optimization. *CoRR*, abs/1402.0796, 2014. URL <http://arxiv.org/abs/1402.0796>.
- Jing Lei, Max G’Sell, Alessandro Rinaldo, Ryan J. Tibshirani, and Larry Wasserman. Distribution-free predictive inference for regression. *Journal of the American Statistical Association*, 113(523):1094–1111, 2018.
- Yaniv Romano, Evan Patterson, and Emmanuel J. Candès. Conformalized quantile regression. In *Neural Information Processing Systems*, 2019.

Glenn Shafer and Vladimir Vovk. A tutorial on conformal prediction. *Journal of Machine Learning Research*, 9(12):371–421, 2008. URL <http://jmlr.org/papers/v9/shafer08a.html>.

Jasper Snoek, Hugo Larochelle, and Ryan P. Adams. Practical bayesian optimization of machine learning algorithms. In F. Pereira, C.J. Burges, L. Bottou, and K.Q. Weinberger, editors, *Advances in Neural Information Processing Systems*, volume 25. Curran Associates, Inc., 2012. URL <https://proceedings.neurips.cc/paper/2012/file/05311655a15b75fab86956663e1819cd-Paper.pdf>.

Kevin Swersky, Jasper Snoek, and Ryan P. Adams. Multi-task bayesian optimization. In C.J. Burges, L. Bottou, M. Welling, Z. Ghahramani, and K.Q. Weinberger, editors, *Advances in Neural Information Processing Systems*, volume 26. Curran Associates, Inc., 2013. URL <https://proceedings.neurips.cc/paper/2013/file/f33ba15effa5c10e873bf3842afb46a6-Paper.pdf>.

Ryan Turner, David Eriksson, Michael McCourt, Juha Kiili, Eero Laaksonen, Zhen Xu, and Isabelle Guyon. Bayesian optimization is superior to random search for machine learning hyperparameter tuning: Analysis of the black-box optimization challenge 2020. In Hugo Jair Escalante and Katja Hofmann, editors, *Proceedings of the NeurIPS 2020 Competition and Demonstration Track*, volume 133 of *Proceedings of Machine Learning Research*, pages 3–26. PMLR, 06–12 Dec 2021. URL <https://proceedings.mlr.press/v133/turner21a.html>.

Martin Wistuba, Nicolas Schilling, and Lars Schmidt-Thieme. Hyperparameter search space pruning – a new component for sequential model-based hyperparameter optimization. In Annalisa Appice, Pedro Pereira Rodrigues, Vítor Santos Costa, João Gama, Alípio Jorge, and Carlos Soares, editors, *Machine Learning and Knowledge Discovery in Databases*, pages 104–119, Cham, 2015. Springer International Publishing. ISBN 978-3-319-23525-7.

## Appendix A.

Search Mode	Average Validation Accuracy	Best Validation Accuracy	Batch CI* Breach Rate	Runtime per Search Iteration	Number of Search Iterations
<b>LW GBM</b>	79.25%	82.74%	15.17%	10.3	145
<b>LW RF</b>	79.99%	82.78%	10.34%	10.2	145
<b>QR GBM</b>	76.84%	82.85%	27.41%	10.8	135
<b>RS</b>	78.62%	82.61%		10.8	139

Table A1: Performance metrics for DNN model tuned on CENSUS data through either PCHO or random search (RS). All PCHO variants are trained at 80% confidence.

\*CI = Conformal Interval

Search Mode	Average Validation Accuracy	Best Validation Accuracy	Batch CI* Breach Rate	Runtime per Search Iteration	Number of Search Iterations
<b>LW GBM 20%</b>	69.35%	77.37%	87.73%	23.5	611
<b>LW GBM 80%</b>	67.86%	77.37%	26.85%	20.9	555
<b>RS</b>	69.09%	77.37%		11.8	1225

Table A2: Performance metrics for DNN model tuned on TSA data through either PCHO or random search (RS). PCHO variants are trained at either 20% or 80% confidence.

\*CI = Conformal Interval

Dataset	Search Mode	Average Validation Accuracy	Best Validation Accuracy	Batch CI* Breach Rate	Runtime per Search Iteration
<b>MNIST</b>	<b>LW GBM</b>	99.39%	97.77%	91.67%	746.4
	<b>RS</b>	99.30%	82.80%		774.0
<b>FMNIST</b>	<b>LW GBM</b>	91.54%	85.95%	87.74%	672.8
	<b>RS</b>	90.86%	73.81%		998.8
<b>CIFAR10</b>	<b>LW GBM</b>	76.09%	70.69%	82.76%	1241.2
	<b>RS</b>	75.52%	42.80%		1084.81

Table A3: Performance metrics for CNN model tuned on suite of CNN datasets (MNIST, FMNIST, CIFAR10) through either PCHO or random search (RS). All PCHO variants are trained at 20% confidence.

\*CI = Conformal Interval